

Supplemental Materials for

**Correlating Hydrogen Evolution Reaction Activity in Alkaline
Electrolyte to Hydrogen Binding Energy on Monometallic Surfaces**

Wenchao Sheng,^a MyatNoeZin Myint,^a Jinguang G. Chen,^{b} and Yushan Yan^{a*}*

[†]Department of Chemical and Biomolecular Engineering

University of Delaware, 150 Academy Street, Newark, DE 19716

[§]Department of Chemical Engineering

Columbia University, 500 West 120th Street, New York, NY 10027

Corresponding Authors:

Jinguang G. Chen: jc3972@columbia.edu

Yushan Yan: yanys@udel.edu

S1. Hydrogen evolution reaction (HER) on monometallic surfaces using the linear sweep voltammetry (LSV)

The HER measurements were performed in 0.1 M KOH prepared from KOH pellets (99.99% trace metals basis, Sigma Aldrich) using de-ionized water (17.5 M Ω ·cm). Prior to the HER measurements, the metal disk electrodes (5 mm in diameter, Pine Instruments) were polished with 0.05 μ m alumina powder, cleaned with de-ionized water, and then mounted onto a rotator (Pine Instruments) as the working electrode. Two spiral Pt wires (Pine Instruments) served as the reference and counter electrodes respectively. With H₂ bubbling throughout the HER measurements, the potential was indeed on the reversible hydrogen electrode (RHE) scale. The polarization curves were taken using LSV, scanning from 0 vs. RHE (−0.2 V for W and −0.1 V for Fe) to a negative potential at a sweep rate of 10 mV/s and a rotation speed of 2500 rpm, which was applied to remove the H₂ bubbles generated during the HER. The LSVs were repeated for a few times until the steady state was reached. The steady state LSVs after solution resistance (iR) correction (see below for the measurement of the cell resistance) were used for data analysis of the HER. However, due to the strong hydrogen absorption property of Ni, Co and Pd, the LSVs kept degrading, and therefore the first LSVs without obvious oxide reduction peaks were used because they closely resemble the metal surface response to the HER. For the measurements of the HER on different metal electrodes, a fresh electrolyte was used and the measurement for each metal disk was within 20 minutes to minimize the contamination from glass corrosion in the alkaline solution. Representative HER LSVs before and after iR-correction of Au and extrapolation of the Tafel plot to the reversible hydrogen potential are shown in Fig. S1.

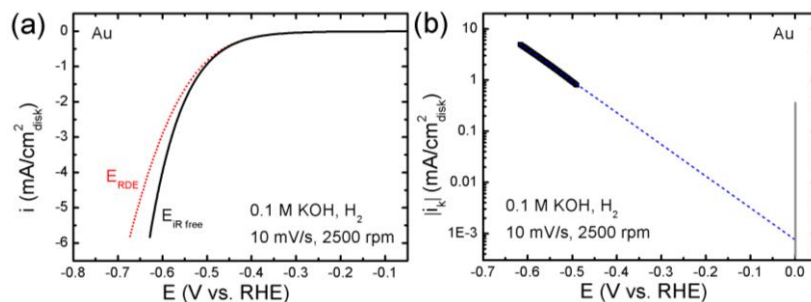


Figure S1. (a) Polarization curve of the HER before (dotted red line) and after (solid black line) solution resistance (iR) correction on Au in H_2 -saturated 0.1 M KOH at room temperature. The data were collected at a sweep rate of 10 mV/s and a rotation rate of 2500 rpm. (b) Tafel plot of the HER on Au (solid black line) and its linear fit and extrapolation to the hydrogen reversible potential (dashed blue line).

S2. HER/HOR on Pt using the rotating disk electrode (RDE) method

The HER/HOR measurement of Pt was taken in the same setup except that a double-junction Ag/AgCl (3.5 M KNO_3) electrode (Analytical Sensor Inc.) was used as the reference electrode, but the potential was referenced to RHE in this paper. The HER/HOR polarization curves were recorded from ~ -0.05 V to ~ 1.0 V vs. RHE at a sweep rate of 10 mV/s and a rotation speed of 2500 rpm. After iR -correction, the kinetic current of the HER/HOR, i_k , was calculated based on the Koutecky-Levich equation

$$\frac{1}{i} = \frac{1}{i_k} + \frac{1}{i_D} \quad (1)$$

where i is the measured current and i_D is the limiting current.¹ Subsequently, the kinetic currents of the HER/HOR were fitted to the Butler-Volmer equation to obtain the exchange current at 0 vs. RHE.

$$i_k = i_0 \left[e^{\frac{\alpha_a F}{RT} \eta} - e^{\frac{-(1-\alpha_a) F}{RT} \eta} \right] \quad (2)$$

In Eq (2), i_0 is the exchange current, α_a is the transfer coefficient, F is the Faraday's constant (96485 C/mol), R is the universal gas constant (8.314 J/mol/K), T is temperature and η is the overpotential.² i_0 values with the best fitting were used in the data analysis.

S3. Electrochemical surface area (ESA) measurements using cyclic voltammetry and capacitance methods

The ESA measurements were made in Ar-saturated 0.1 M KOH solution (prepared from KOH pellets, Sigma Aldrich, with de-ionized water). A double junction Ag/AgCl (3.5 M KNO₃) electrode and a spiral Pt wire served as the reference and counter electrodes respectively. All the potentials were referenced to the RHE scale.

Pt: The CV was scanned from ~0.03V to 1.0 V vs. RHE at a sweep rate of 50 mV/s. The hydrogen adsorption/desorption region between 0.05 V and ~0.4 V vs. RHE (the onset of the double layer region) was used to calculate the Pt surface area, assuming a charge density of 210 $\mu\text{C}/\text{cm}^2_{\text{Pt}}$ for one monolayer of hydrogen coverage.^{3,4}

Ni: The CV was scanned from ~ -0.15 to ~ 0.56 V vs. RHE at a sweep rate of 50 mV/s. The reduction peak at ~ 0.05 V vs. RHE corresponds to the reduction of Ni(OH)₂. The charge density is $514 \mu\text{C}/\text{cm}^2_{\text{Ni}}$.^{5,6}

Ag: The CV was scanned from ~ 0 to ~ 1.6 V vs. RHE at a sweep rate of 100 mV/s. The peak at ~ 1.25 V vs. RHE can be attributed to the formation of one monolayer of AgOH or Ag₂O, which corresponds to a charge density of $\sim 400 \mu\text{C}/\text{cm}^2_{\text{Ag}}$.⁷

Cu: The CV was scanned from ~ -0.5 V to ~ 1.65 V vs. RHE at a sweep rate of 20 mV/s. The broad anodic peak between ~ 0.5 V and ~ 0.71 V corresponds to the formation of one monolayer of Cu₂O with a charge density of $360 \mu\text{C}/\text{cm}^2_{\text{Cu}}$.⁸

Au: The CV was scanned from ~ 0 to ~ 1.6 V vs. RHE at a sweep rate of 100 mV/s. The reduction peak centered at ~ 1.1 V is due to the reduction of AuO, which corresponds to a charge density of $390 \mu\text{C}/\text{cm}^2_{\text{Au}}$.⁹

Pd: The CV was scanned from ~ 0.16 V to ~ 1.25 V vs. RHE at a sweep rate of 50 mV/s. The oxide reduction peak located at ~ 0.75 V corresponds to a charge density of $424 \mu\text{C}/\text{cm}^2_{\text{Pd}}$.¹⁰ All the CVs are shown in Fig. S2.

Co: The ESA of Co was determined using specific capacitance method. The CVs were recorded in Ar-saturated 0.1 M KOH at sweep rates of 10, 20, 30, 40, and 50 mV/s between 0.87 V and 0.97 V vs. RHE. The current densities (per geometric surface area) at 0.92 V were plotted as a function of the scanning rate. The slope of the straight line, divided by the specific capacitance ($60 \mu\text{F}/\text{cm}^2$),¹¹ gives the roughness factor of the electrode (Fig. S3). The real surface area was then calculated by geometric area (5 mm in diameter) times the roughness factor.

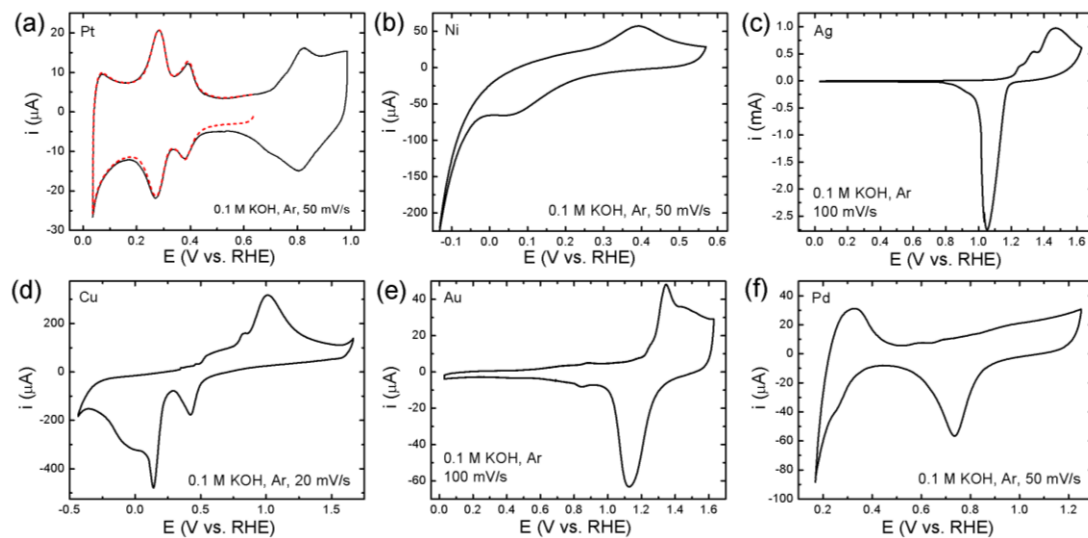


Figure S2. (a) Cyclic voltammograms (CVs) of (a) Pt with two different upper potential limits, (b) Ni, (c) Ag, (d) Cu, (e) Au and (f) Pd in Ar-saturated 0.1 M KOH.

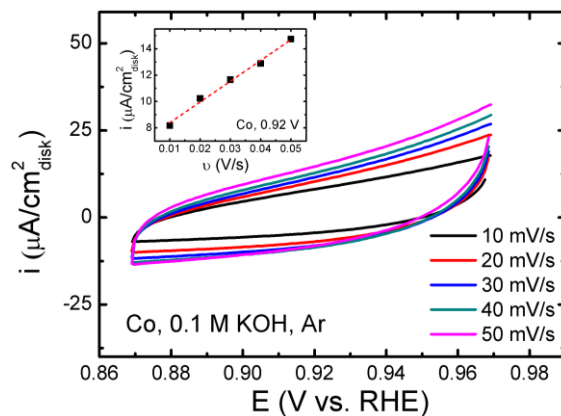


Figure S3. CVs of Co in Ar-saturated 0.1 M KOH at different sweep rates. The inset shows the linear relationship between the current density and the sweep rate at 0.92 V. The roughness factor of the Co surface can be calculated by dividing the slope by the specific capacitance of Co.

S4. Impedance measurements

The solution resistances were measured right after the LSV measurements of the HER at a constant potential with a 10 mV voltage perturbation applied. The ac spectra were taken from 200 kHz to 1 Hz, where the real part of the resistance at 1 kHz was used as the solution resistance.¹² The HER/HOR polarization curves were then corrected to obtain iR-free potential of the working electrode.

References

1. A. J. Bard and L. R. Faulkner, in *Electrochemical Methodes: Fundamentals and Applications*, John Wiley & Sons, New York, 2001, p. 341.
2. A. J. Bard and L. R. Faulkner, in *Electrochemical Methodes: Fundamentals and Applications*, John Wiley & Sons, New York, 2001, p. 103.
3. F. C. Nart and W. Vielstich, *Handbook of Fuel Cells: Fundamentals, Technology and Applications*, John Wiley & Sons, New York, 2003.
4. T. J. Schmidt, H. A. Gasteiger, G. D. Stab, P. M. Urban, D. M. Kolb and R. J. Behm, *J Electrochem Soc*, 1998, **145**, 2354-2358.
5. B. E. Conway and L. Bai, *J Chem Soc Farad T 1*, 1985, **81**, 1841-&.
6. S. A. S. Machado and L. A. Avaca, *Electrochim Acta*, 1994, **39**, 1385-1391.
7. J. G. Becerra, R. C. Salvarezza and A. J. Arvia, *Electrochim Acta*, 1988, **33**, 1431-1437.
8. S. Fletcher, R. G. Barradas and J. D. Porter, *J Electrochem Soc*, 1978, **125**, 1960-1968.
9. S. Trasatti and O. A. Petrii, *Pure Appl Chem*, 1991, **63**, 711-734.
10. D. A. J. Rand and R. Woods, *J Electroanal Chem*, 1971, **31**, 29-&.
11. B. S. Yeo and A. T. Bell, *J Am Chem Soc*, 2011, **133**, 5587-5593.
12. W. C. Sheng, H. A. Gasteiger and Y. Shao-Horn, *J Electrochem Soc*, 2010, **157**, B1529-B1536.